Performance of self-healing epoxy with microencapsulated healing agent and shape memory alloy wires

E.L. Kirkby [a], V.J. Michaud [a], J.-A.E. Månson [a,*], N.R. Sottos [b], S.R. White [b]

[a] Laboratoire de Technologie des Composites et Polymères, Institut des Matériaux, Ecole Polytechnique Fédérale de Lausanne, CH-1015 Lausanne, Switzerland
[b] Autonomic Materials Systems Group, Beckman Institute for Advanced Science and Technology, University of Illinois at Urbana-Champaign, Urbana, IL 61801, USA

ARTICLE INFO

ABSTRACT

We report the first measurements of a self-healing polymer that combines a microencapsulated liquid healing agent and shape memory alloy (SMA) wires. When a propagating crack ruptures the embedded microcapsules, the liquid healing agent is automatically released into the crack where it contacts a solid catalyst embedded in the matrix. The SMA wires are then activated to close the crack during the healing period. We show that dramatically improved healing performance is obtained by the activation of embedded SMA wires. We conclude that improved healing is due to a reduction of crack volume as a result of pulling the crack faces closed, and more complete polymerization of the healing agent due to the heat produced by the activated SMA wires.

1. Introduction

Damage to engineering materials in service eventually causes them to wear out or fail. Until recently, the only solution was manual repair or replacement of the damaged component. However, new materials that self-heal are now being developed. Self-healing composites could be especially important for the aerospace sector, for example, in cases where internal damage is difficult to detect, or where it is impossible to carry out field repairs. Automatic repair during service would also provide more reliable and safer aerospace structures.

The first self-healing polymer was reported by White et al. [1], based on a liquid healing agent (dicyclopentadiene, DCPD) contained in urea–formaldehyde (UF) microcapsules [2] and a solid catalyst (Grubbs' first generation catalyst), both dispersed in an epoxy matrix. In this material, a propagating crack ruptures the microcapsules in its path, releasing the low-viscosity healing agent, which then covers the crack plane by capillary action and polymerizes on contact with the catalyst via ring-opening metathesis polymerization (ROMP). Since the first demonstration, the microencapsulation system has been developed further and optimized. For example, smaller capsule sizes [3,4], improved catalysts [5,6] and alternative healing systems [7,8] have been investigated. In a separate approach to the delivery system, Trask et al. embed hollow glass fibers in a composite material, infused with either resin or curing agent (Cycom 823 two-part system) [9,10]. The fibers rupture on impact, releasing the components into the damaged region. Toohey et al. have shown that delivery of healing agents via a microvascular network will enable multiple healing events [11].

The materials system reported in this paper is based on the White et al. microcapsule approach [1]. Following established protocols [12,13], the performance is evaluated by measuring the peak load required to re-fracture a tapered double cantilever beam (TDCB) sample, after healing. In previous studies [3,13] we have shown that the healing performance depends on the fill factor (γ) [13], defined as:

$$\gamma = \frac{V_h}{V_c} \qquad (1)$$

where V_h and V_c are the volume of the delivered healing agent and of the closed crack, respectively. For optimum healing, $\gamma > 1$ and the healed peak load is maximum. For epoxy healed at room temperature, the healing efficiency peaks at about 50% with respect to the virgin material [3]. However, the healed peak load drops off rapidly when $\gamma < 1$. A technique is therefore needed to minimize the crack volume and ensure optimal healing even with small amounts of delivered healing agent.

Shape memory alloy (SMA) wires can provide this function in a self-healing material. In a previous study [13] SMA wires bridging a crack were activated during healing, exerting a closure force of several Newtons per wire. Samples containing SMA wires that were manually injected with DCPD healing agent showed an increase in average healed peak fracture load from about 38 N to 60 N,

corresponding to an increase of healing efficiency from 49% to 77%. The improvement in healing efficiency is due to the reduced crack volume and to heating of the SMA wires during activation. In this paper we report that comparable improvements in healing performance are observed with SMA wires when the healing agent is delivered autonomically from microcapsules.

2. Experimental methods

2.1. Microcapsule thermal stability

Microcapsules containing DCPD healing agent were fabricated as described in Ref. [2]. Their thermal stability was assessed by thermogravimetric analysis (TGA). Samples of microcapsules (10–20 mg) were weighed in a 150 µl ceramic crucible and then placed in the TGA. The TGA was heated from 25 °C to 600 °C at a rate of 10 °C/min, under a controlled nitrogen environment, while continuously monitoring the sample mass.

2.2. Fracture behavior of polyDCPD healing agent

The fracture behavior of polyDCPD was evaluated by compact tension (CT) testing following ASTM standard D 5045–91a (Fig. 1). To prepare the samples, DCPD was mixed with 5 wt% Grubbs' catalyst wax microspheres (containing 10 wt% catalyst and 90 wt% wax) and cast in an aluminum mold to form a polymer plate. Two types of samples were prepared to simulate the different types of healing cycles. The first plate was allowed to polymerize at room temperature for 24 h. The second plate was placed in an oven at 80 °C for the first 30 min after mixing to simulate the effects of the heating cycle of the SMA wires (§2.3), and then left at room temperature for 24 h.

Four CT samples were machined from each plate. Each sample notch was sharpened by scoring with a razor blade, forming a precrack. The pre-crack length was measured for each sample, and was typically 0.1–0.3 mm. The samples were then individually mounted in a tensile tester and loaded in tension at a constant displacement rate of 5 µm/s, 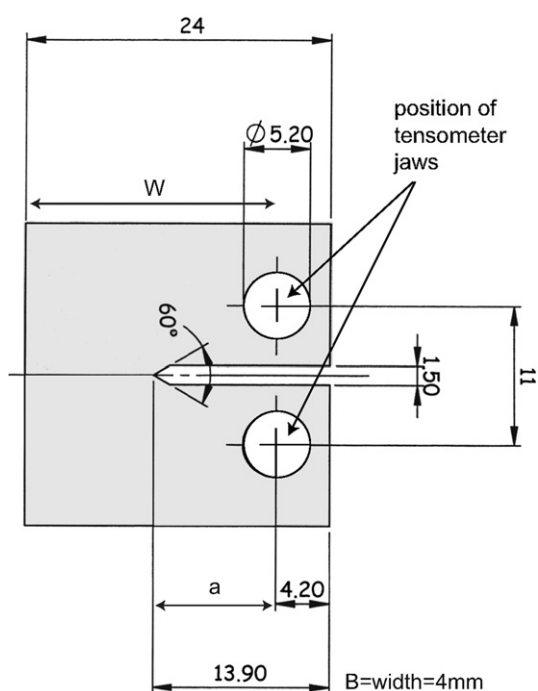until failure, recording the force, P (N) as a function of time. The characteristics of the force–displacement plots of the two sample types were then compared. The fracture characteristics of the two sample types were also compared with scanning electron microscope (SEM) images of the fracture planes.

For the samples that followed linear elastic fracture mechanics, the fracture toughness, K_{IC} (MPa m$^{1/2}$), was calculated from the expression:

$$K_{IC} = \frac{P_C}{BW^{1/2}} f(x) \qquad (2)$$

where, P_C (N) is the critical load for crack propagation, B (m) is the sample width, W (m) is the distance between the centre of the loading slot and the back end of the sample, and

$$f(x) = \frac{(2+x)(0.886 + 4.64x - 13.32x^2 + 14.72x^3 - 5.6x^4)}{(1-x)^{3/2}} \qquad (3)$$

where $x = a/W$, $0.2 < x < 0.8$ and a includes the length of the precrack.

2.3. Healing performance of SMA/microcapsule self-healing epoxy

For all self-healing tests the matrix material was EPON 828 resin (Shell Chemicals) cured with diethylenetriamine (DETA; Sigma–Aldrich) in a 100:12 mass ratio. The properties of the SMA wires (Furukawa Electric) are summarized in Table 1. The transformation temperatures were determined by differential scanning calorimetry.

The self-healing properties were investigated using samples with a tapered double cantilever beam (TDCB) geometry (Fig. 2), first developed by Mostovoy et al. [14]. This technique provides a measurement of the fracture toughness that is independent of the initial crack length, i.e.

$$K_{IC} = \alpha P_C \qquad (4)$$

where $\alpha = 11.2 \times 10^3$ m$^{-3/2}$ for the present geometry [12]. Three SMA wires were each tensioned with a 50 g mass and embedded at the mid-plane of the sample, perpendicular to the crack direction (Fig. 2). Microcapsules of typically 100–200 µm diameter were prepared, containing DCPD healing agent [2]. The microcapsules were added into the epoxy matrix in a 5, 10 or 20 wt% concentration. Grubbs' first generation catalyst (Sigma–Aldrich) was recrystallized via a non-solvent addition method [15] and wax-encapsulated for protection [5], to form 10 wt% Grubbs' catalyst in wax microspheres of 200 µm average size. The microspheres were added into the epoxy matrix in a 5 wt% concentration. In order to minimize costs, the microspheres were localized around the crack plane region (Fig. 2) [3]. The resin was degassed, cured in silicone rubber molds for 24 h at room temperature, and post-cured at 35 °C for a further 24 h. After post-curing, a sharp pre-crack was made by tapping a razor blade into the molded starter-notch.

Fig. 1. Compact tension (CT) sample geometry (distance units are mm).

Table 1
Properties of the SMA wires used in the present study. M_s and M_f are the start and finish temperatures, respectively, of the martensite-to-austenite (forward) transformation. A_s and A_f are the corresponding temperatures of the austenite-to-martensite (reverse) transformation.

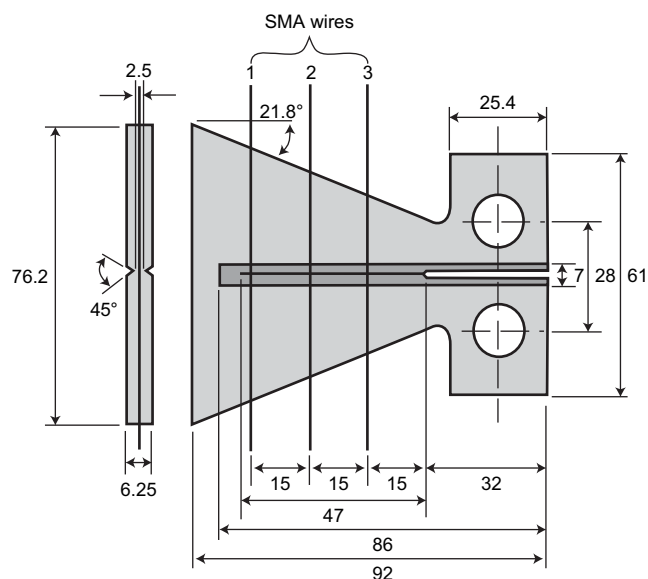| Composition (Ni:Ti:Cu)	44.86:45.08:10.06
Diameter	150 µm
M_s	53.6 °C
M_f	47.1 °C
A_s	59.8 °C
A_f	65.6 °C

Fig. 2. The tapered double cantilever beam (TDCB) geometry. Samples were prepared both without SMA wires and with three SMA wires perpendicular to the crack plane, spaced uniformly. The 7 mm-wide region around the crack plane indicates where Grubbs' catalyst was localized. The distance units are mm.

The TDCB samples were mounted in a load frame with two pins and loaded in tension at a constant displacement rate of 5 μm/s. At failure, a crack propagated horizontally along the side-grooves, along the full length of the specimen, fracturing the sample into two halves and releasing the healing agent from the microcapsules. The SMA wires have a tensile strength of 1.34 GPa, and a maximum elongation of 13% before failure, so the wires remained intact when the sample failed. The peak load at failure was recorded, from which the virgin fracture toughness was calculated Eq. (4).

The two sample halves were then removed together from the load frame. Following this, the SMA wires were mechanically clamped at the points where they exited the TDCB samples. This was achieved by placing them between two aluminum plates with dimension of 70 mm by 20 mm, which were then clamped together using nuts and bolts. This eliminated any influence of the quality of the SMA interfacial bonding on the present measurements. The SMA wires were then activated for 30 min with a DC current of 0.5 A per wire. During activation, the temperature of the wires and local matrix reached 80 °C and each wire generated an axial recovery force of 4.5 N (240 MPa axial stress) which acted to close the crack faces [13]. Following the activation period, the SMA clamps were removed and the sample was left at room temperature for 24 h.

After healing, the crack face separation of each sample was determined using an optical microscope. The SMA wires were carefully debonded by manually applying a force to them, and fully removed from the matrix. The samples were then re-tested to failure under the same conditions as for the virgin material, and the healed peak load recorded. The self-healing performance of a material can be quantified by the healing efficiency [12]:

$$\eta = \frac{K_{IC_H}}{K_{IC_V}} = \frac{P_{C_H}}{P_{C_V}} \tag{5}$$

where K_{IC_V} and K_{IC_H} are the virgin and healed fracture toughness, respectively, and P_{C_V} and P_{C_H} are the virgin and healed peak loads at fracture, respectively. However, the virgin fracture toughness depends on microcapsule size and concentration [16], and so η does not reflect the healing performance alone. Therefore, in this paper we follow a method presented by Rule et al. in Ref. [3], in which healing performance is evaluated by directly comparing the healed peak loads.

2.4. Fill factor determination

The fill factor of each sample was determined as follows. The amount of healing agent delivered per unit crack area, D_h (g cm^{-2}), is given by:

$$D_h = \rho_m \phi d_c \tag{6}$$

where ρ_m is the density of the matrix (1.16 g cm^{-3}), ϕ is the weight fraction of microcapsules and d_c (cm) is the diameter of the microcapsules [3]. The volume of delivered healing agent is then $V_h = D_h A / \rho_h$, where A (cm^2) is the crack area and ρ_h is the density of
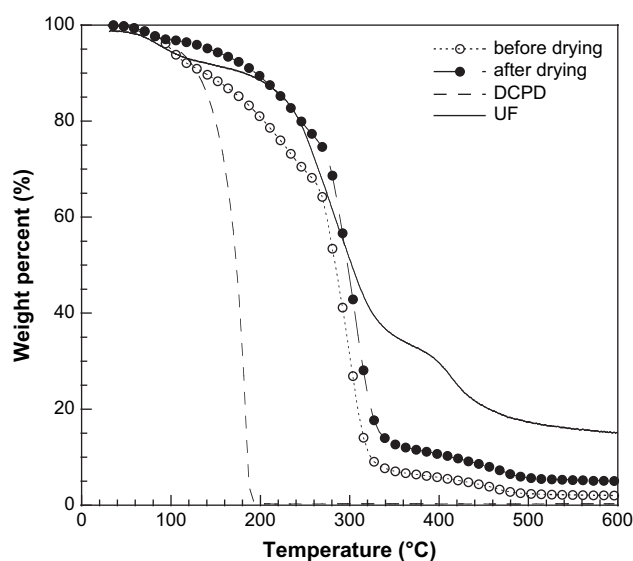

Fig. 3. Measurement of the normalized weight versus temperature of samples of microcapsules and their components: (a) microcapsules without prior drying to remove water (hollow circles), (b) pre-dried microcapsules (solid circles), (c) dicyclopentadiene (dashed line), and (d) urea–formaldehyde shell wall (solid line). Each sample initially weighed around 10–20 mg and the heating rate was 10 °C/min.
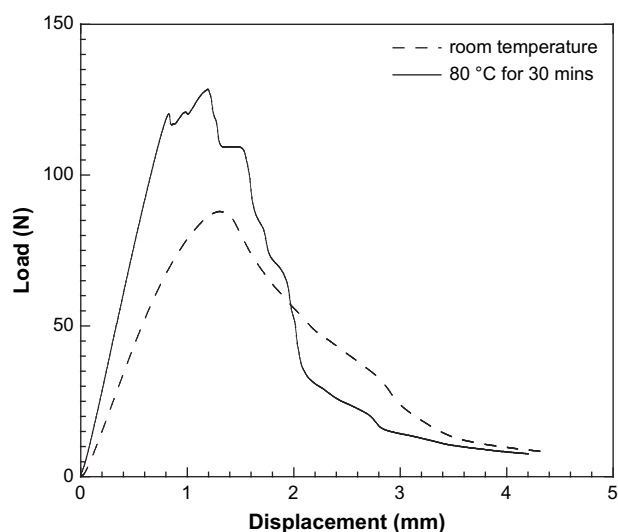

Fig. 4. Representative load versus displacement compact tension results of polyDCPD after polymerization either (a) at room temperature for 24 h or (b) at 80 °C for 30 min followed by 24 h at room temperature.
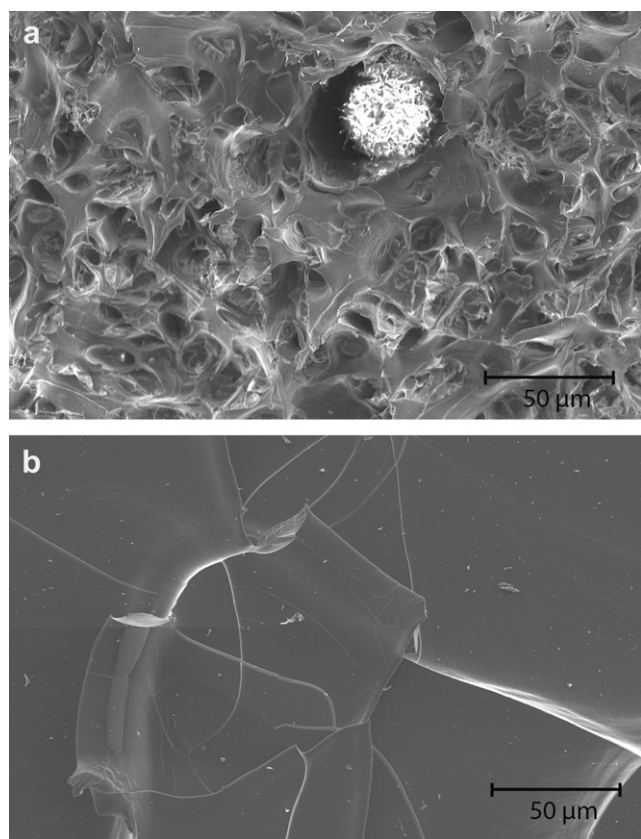
Fig. 5. Scanning electron microscope images of the fracture surface of the polyDCPD after polymerization for (a) 24 h at room temperature (20 °C; the circular feature toward the top center is an undissolved catalyst/wax microsphere) and (b) 30 min at 80 °C, followed by 24 h at room temperature (20 °C). The fracture surface of the room temperature sample is highly textured, with evidence of tearing and plastic deformation, while the surface of the 80 °C cured sample is smooth and glass-like, indicating a brittle fracture.

DCPD (0.98 g cm^{-3}). The crack volume is $V_c = A \cdot w$ where w (cm) is the crack separation, as measured by optical microscopy. The fill factor is then given by:

$$\gamma = \frac{V_h}{V_c} = \frac{\rho_m \phi d_c}{\rho_h w} \tag{7}$$

3. Results and discussion

3.1. Microcapsule thermal stability

Typical weight loss curves for microcapsules and components are presented in Fig. 3. DCPD monomer rapidly loses weight between 150 and 180 °C, corresponding to its boiling point (170–172 °C). However, when DCPD is encapsulated in a UF shell wall, rapid weight loss does not occur until 300 °C—the temperature at which the UF shell wall begins to degrade. These observations confirm that the microcapsules were predominantly well-formed and robust.

Although the rapid weight loss of the microcapsule samples occurs near 300 °C, a gradual decrease in mass is observed between 100 and 280 °C. Comparing capsules that were pre-dried with those that were not, there is clear evidence that part of the weight loss in this interval is due to evaporation of residual water. In addition, the UF shell material samples also show loss in mass over the same temperature range, suggesting that some weight loss may be due to evaporation of high volatility compounds from the UF walls. Since TGA measurements are performed on batch samples, some (small) fraction of microcapsules that is poorly formed could also lead to premature weight loss. Nevertheless, over the temperature range of interest (<80 °C) these microcapsules retain the vast majority of their content.

3.2. Fracture behavior of polyDCPD healing agent

A total of eight compact tension samples of DCPD polymerized with 5 wt% Grubbs' catalyst wax microspheres (containing 10 wt% Grubbs' catalyst and 90 wt% wax) were prepared and tested. Of these, four were polymerized at room temperature for 24 h, while the other four were initially placed in an oven at 80 °C for 30 min. Fig. 4 shows representative load–displacement results for each sample type. The samples polymerized at room temperature exhibited non-linear fracture behavior, indicative of incomplete polymerization, with an average fracture load of 89.0 ± 3.1 N. The samples polymerized at 80 °C exhibited linear elastic fracture characteristics, with an average fracture load of 123.0 ± 3.3 N, corresponding to a fracture toughness of 2.08 ± 0.06 MPa m$^{1/2}$ Eq. (2).

In addition to an increased fracture load, the samples polymerized at 80 °C exhibited a more brittle fracture behavior. The load–displacement curve in Fig. 4 is linear up to the fracture point in comparison to the samples polymerized at room temperature. Fig. 5 shows SEM images of the fracture surfaces of the two samples, taken with a Philips XL30 ESEM-FEG. The fracture surface of the room temperature sample is highly textured, with evidence of tearing and plastic deformation. In contrast, the fracture surface of the 80 °C sample is smooth and glass-like, with relatively little texture. These SEM images support the findings in Fig. 4 and reinforce the conclusion that the heating effect of the SMA wires contributes significantly to the overall healing performance. However, no direct correlation between the properties of the bulk polyDCPD and the polyDCPD film formed in situ in TDCB samples can be drawn. Fracture toughness and associated mechanical performance are inherently dependent on the concentration of catalyst and the polymerization temperature—two quantities that are uncontrolled during in situ healing. The measurements presented in this section therefore serve only as an indication of the influence of heating on the fracture behavior.

3.3. Influence of SMA wires on virgin fracture toughness

In order to isolate the effect of SMA wires on healing performance it was first necessary to investigate their influence on the fracture

Table 2
Effect of SMA wires on the virgin matrix peak load and fracture toughness, K_{IC}. The values without SMA wires were obtained by Rule et al. [3] Grubbs' catalyst was located around the crack plane region (Fig. 2).

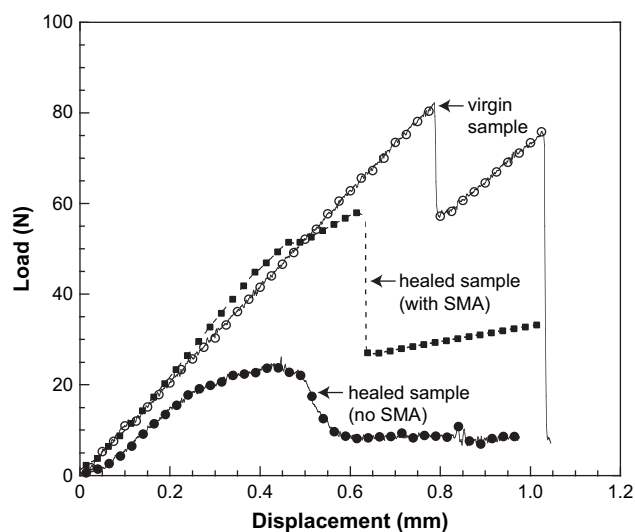| Sample	With SMA wires		Without SMA wires	
	Virgin peak load [N]	K_{IC} [MPa m$^{1/2}$]	Virgin peak load [N]	K_{IC} [MPa m$^{1/2}$]
Epoxy	68.6	0.77 ± 0.10	77.7	0.87 ± 0.12
Epoxy/Grubbs' (5 wt%)/ localized capsules	131.7	1.47 ± 0.15	123.2	1.38 ± 0.10
Epoxy/Grubbs' (5 wt%)/non-localized capsules	95.4	1.07 ± 0.12	96.4	1.08 ± 0.15

Fig. 6. Representative curves of load versus displacement for TDCB samples containing 20 wt% microcapsules: (a) virgin sample, (b) healed sample without SMA wires (fill factor ~0.6), and (c) healed sample with SMA wires (fill factor 1.7).

toughness of the virgin epoxy material. We previously found that the SMA wires have no influence on the virgin fracture toughness of pure epoxy samples [13]. Here we determine if the same conclusions can be drawn for samples containing microcapsules. TDCB samples were prepared as described in §2. The mean peak loads of the virgin samples, and their corresponding fracture toughness, are summarized in Table 2. The values for the samples with and without SMA wires are within one standard deviation of one another for all three sample types. Thus, any improved self-healing performance reported here is due to improved healing of the crack—and not to any toughening effect of the embedded SMA wires.

It is interesting to note that the intrinsic virgin fracture toughness of bulk polyDCPD healed at 80 °C ($\sim$2.0 MPa m$^{1/2}$, §3.2) is higher than that of the self-healing epoxy matrix with embedded Grubbs' catalyst microspheres and non-localized capsules (Table 2). This implies that when the healed TDCB sample is re-tested, the crack could propagate along the interface between the original crack plane and the film of polyDCPD and, with sufficient adhesion, could branch into new (virgin) material where the microcapsules are still intact, allowing further healing to take place. However, as highlighted in §3.2, there are significant differences between the bulk and film polyDCPD, and so further tests would be necessary to draw a conclusion.

3.4. Healing performance

TDCB samples containing microcapsules both with and without SMA wires were prepared and then fractured, healed and re-fractured as described in §2. Representative results of both are shown in Fig. 6. For samples without SMA wires our results are compared

Table 3
Comparison of our measurements with those of Rule et al. [3] for TDCB samples containing microcapsules, but no SMA wires. The diameter of the microcapsules in the Kirkby samples was 114 ± 6 μm.

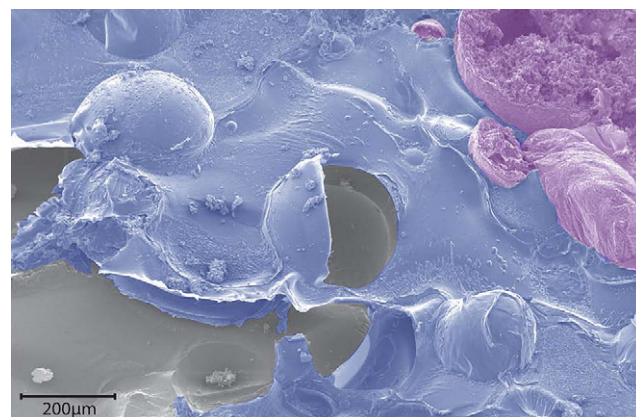| Capsule concentration [wt%]	Healing agent delivered [mg cm^{-2}]	Healed peak load [N]	
		Kirkby	Rule universal curve
5	0.66	4.7 ± 1.1	8.0
10	1.32	8.8 ± 1.6	12.0
20	2.64	18.4 ± 2.6	24.5

Fig. 7. Crack plane image of a well-healed microcapsule/SMA sample with 20 wt% microcapsule loading in the matrix. The polyDCPD film (highlighted in blue) covers most of the imaged surface. A Grubbs' catalyst wax microsphere is present in the top right corner of the image (highlighted in purple). (For interpretation of the references to color in this figure legend, the reader is referred to the web version of this article.)

directly to those of Rule et al. [3] in Table 3; the curve for the sample healed without SMA wires in Fig. 6 is one such measurement. It should be noted that this particular healing event does not represent the maximum room temperature healing performance; the fill factor of this specific sample was 0.6, and was chosen so that our results could be directly compared to those by Rule et al. in Ref. [3]. The maximum healed peak load for room temperature samples, achieved when the fill factor is at least unity, is about 40 N [13], corresponding to a healing efficiency of about 50%. The two sets of measurements of healed peak load in Table 3 are in reasonable agreement, although ours are systematically about 25–30% lower. One possible explanation is that we have used larger catalyst microspheres for these particular measurements (510 ± 10 μm versus 220 μm for Rule et al.), which would alter the dissolution kinetics of the catalyst in the DCPD.

For TDCB samples containing both SMA wires and microcapsules the healed response displays a linear elastic brittle-type fracture, similar to the virgin response (Fig. 6). The sample without SMA wires exhibits a more plastic-like fracture, indicative of incomplete polymerization when healing at room temperature alone. These
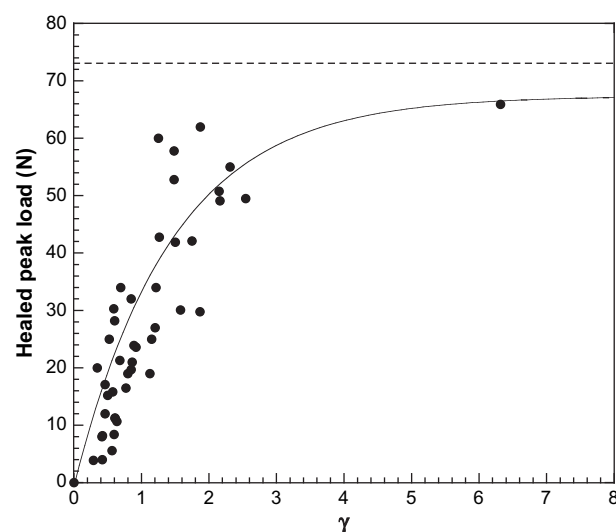

Fig. 8. Peak load versus fill factor for healed TDCB samples with microencapsulated healing agent and SMA wires. The solid curve is a general fit to the data. The dashed line indicates the mean peak load of the virgin samples.

observations are consistent with the observed fracture characteristics of the polyDCPD healing agent (§3.2). The fracture surface of a well-healed sample is shown in Fig. 7, and displays a polyDCPD film that is continuous and crisp-edged, characteristic of a strong heal.

For samples with SMA wires, 20 wt% microcapsules with diameters ranging between 140 and 205 μm were used. The fill factor of the healed samples Eq. (7) varied from about 0.3 to almost 7 in one case, corresponding to crack separations ranging from 185 to 8 μm (58 μm mean and 39 μm standard deviation for all samples). Fill factors above unity indicate that more healing agent is delivered than necessary to fill the crack volume, assuming perfect filling efficiency. In the case of TDCB samples, excess healing agent flows out of the crack plane along the edges of the crack.

Around 40 TDCB samples with microcapsules and SMA wires were tested. The results are shown in Fig. 8. The healed peak load reaches a maximum around 60 N, roughly 80% of the peak load of the virgin material. This represents a 33% increase compared to the room temperature samples of equivalent fill factor, consistent with the results in Ref. [13]. Furthermore, maximum healing is achieved with a lower volume of healing agent when SMA wires are incorporated in the material, as they reduce the crack volume.

4. Conclusion

We have shown that embedding SMA wires that bridge the fracture plane and activating them during the healing process leads to significant improvements in the performance of self-healing polymers with microencapsulated healing agent. These results confirm and support our earlier studies in which the healing agent was injected manually. The improved performance is due to two factors: a decreased crack volume and, consequently, an improved filling efficiency with a given quantity of healing agent; and improved mechanical properties of the polymerized healing agent, due to the heating effect of the SMA wires, which improves cross-linking during polymerization. The relative impacts of these two factors have been previously evaluated in Ref [13]. Furthermore, we find that fill factors of at least two are required to reach the maximum healing efficiency. These results suggest that practical applications should aim for an over-delivery of healing agent of at least a factor of two to ensure complete filling of the crack and the highest healing efficiency.

Acknowledgements

References

[1] White SR, Sottos NR, Guebelle PH, Moore JS, Kessler MR, Sriram SR, et al. Nature 2001;409:794–7.
[2] Brown EN, Kessler MR, Sottos NR, White SR. J Microencapsul 2003;20(6):719–30.
[3] Rule JD, White SR, Sottos NR. Polymer 2007;48:3520–9.
[4] Blaiszik BJ, Sottos NR, White SR. Compos Sci Technol 2008;68:978–86.
[5] Rule JD, Brown EN, Sottos NR, White SR, Moore JS. Adv Mater 2005;17(2):205–8.
[6] Kamphaus JM, Rule JD, Moore JS, Sottos NR, White SR. J R Soc Interface 2008; 5:95–103.
[7] Keller MW, White SR, Sottos NR. Adv Funct Mater 2007;17:2399–404.
[8] Caruso MM, Blaiszik BJ, White SR, Sottos NR, Moore JS. Adv Funct Mater 2008; 18:1898–904.
[9] Trask RS, Bond IP. Smart Mater Struct 2006;15:704–10.
[10] Trask RS, Williams GJ, Bond IP. J R Soc Interface 2007;4:363–71.
[11] Toohey K, Lewis JA, Moore JS, White SR, Sottos NR. Nat Mater 2007;6:581–6.
[12] Brown EN, Sottos NR, White SR. Exp Mech 2002;42(4):372–9.
[13] Kirkby EL, Rule JD, Michaud VJ, Sottos NR, White SR, Månson J-AE. Adv Funct Mater 2008;18:2253–60.
[14] Mostovoy S, Crosley PB, Ripling EJ. J Mater 1967;2:661–81.
[15] Jones AS, Rule JD, Moore JS, White SR, Sottos NR. Chem Mater 2006;18:1312–7.
[16] Brown EN, White SR, Sottos NR. J Mater Sci 2004;39:1703–10.